

Field-tilt anisotropy energy in quantum Hall stripe states

T. Jungwirth

*Department of Physics, Indiana University, Bloomington, Indiana 47405
and Institute of Physics ASCR, Cukrovarnická 10, 162 00 Praha 6, Czech Republic*

A. H. MacDonald

Department of Physics, Indiana University, Bloomington, Indiana 47405

L. Smrčka

Institute of Physics ASCR, Cukrovarnická 10, 162 00 Praha 6, Czech Republic

S. M. Girvin

Department of Physics, Indiana University, Bloomington, Indiana 47405

(Received 2 September 1999)

Recently reported giant anisotropy in the longitudinal resistivity of a two-dimensional (2D) electron system with valence Landau level index $N \geq 2$ has been interpreted as a signal of unidirectional charge density wave (UCDW) ground states. We report on detailed Hartree-Fock calculations of the UCDW orientation energy induced by a tilted magnetic field. We find that for current experimental samples, stripes are oriented perpendicular to the in-plane field, consistent with experiment. For wider 2D electron systems, we predict tilt-induced stripe states with variable anisotropy energy sign. [S0163-1829(99)16047-8]

Several groups¹⁻⁵ have reported the observation of strong anisotropies and nonlinearities in the low-temperature magnetotransport of clean two-dimensional (2D) electron systems over ranges of Landau level (LL) filling factor surrounding $\nu = n + 1/2$ for $n \geq 4$, i.e., for valence LL orbital index $N \geq 2$. Although the origin of these anomalies has not been firmly established, the anisotropy is probably associated with the unidirectional charge density wave (UCDW) UCDW states which have been predicted to occur under precisely these circumstances.^{6,7} Recently Pan *et al.*⁴ and Lilly *et al.*² have discovered that the isotropic gapped $\nu = 5/2$ quantum Hall state gives way to the anisotropic state for sufficiently large in-plane magnetic fields. Shayegan and Manoharan⁵ have observed that in a 2D hole system the $\nu = 5/2$ state is already anisotropic even without in-plane field, indicating that lower electron density (more LL mixing) can stabilize the CDW. Both of these observations are consistent with an anisotropic spontaneously-broken orientational-symmetry state, like the UCDW state. Several recent theoretical papers⁸⁻¹⁰ have explored the properties of these “liquid crystal” states for perpendicular field.

In this paper, we evaluate the dependence of UCDW state’s energy on its orientation relative to the in-plane field component, when the magnetic field is tilted away from the 2D electron system normal. Theoretical studies along similar lines have recently been carried out by two other groups.^{11,12} We find that screening due to polarization of remote LL’s plays an essential role for the preferred orientation of the stripes. Using a realistic model for the sample of Lilly *et al.* (a single GaAs/Al_xGa_{1-x}As heterojunction with density $N_e = 2.67 \times 10^{11} \text{ cm}^{-2}$) we quantitatively determine the anisotropy energy and find that the stripes prefer to be aligned perpendicular to the in-plane field for the whole range of studied field-tilt angles and filling factors, consistent with

experimental observations. The same conclusion was found to apply for the lower density ($N_e = 2.2 \times 10^{11} \text{ cm}^{-2}$) sample of Pan *et al.* To explore the dependence of this result on system geometry we have repeated these calculations for a parabolic confinement quantum well models with variable subband separation. These calculations reveal a mechanism for tilt-induced UCDW states in samples with more than one occupied subband for which the perpendicular field state is expected to be isotropic. We find that stripe orientation parallel to the in-plane field is possible when two subbands are occupied at zero tilt angle.

Our calculation starts from the following observation.^{13,14} The property that states within a LL are related to each other by operations of the magnetic translation group implies equivalence of any LL to the lowest LL of a zero-thickness 2D electron system with a suitably adjusted effective electron-electron interaction. For the example of interest here, a quasi-2D electron system in the $x-y$ plane with the magnetic field tilted away from the normal to the plane,¹⁵ we choose the in-plane component B_{\parallel} of the magnetic field to be in the \hat{x} direction and use the following Landau gauge for the vector potential, $\vec{A} = (0, B_{\perp}x - B_{\parallel}z, 0)$. The one-particle orbitals for any z -dependent single-particle confining potential can then be written as

$$\langle \vec{r} | k, i, \sigma \rangle = \frac{e^{iky}}{\sqrt{L_y}} \varphi_{i,\sigma}(x - l^2 k, z), \quad (1)$$

where k is the wave vector that labels states within LL i , σ is the spin index, and $l^2 = \hbar c / e B_{\perp}$. The translational symmetry responsible for LL degeneracy leads to a 2D wave function $\varphi_{i,\sigma}(x, z)$, which is independent of the state label k , except for the rigid shift by $l^2 k$ along x axis. This in turn leads to

two-particle matrix elements of the Coulomb interactions with a dependence on state labels which is identical to that for the lowest LL of a zero-thickness 2D electron system provided the 2D Coulomb interaction is replaced by the following effective interaction

$$V(\vec{q}) = \frac{4\pi e^2}{\epsilon} e^{q^2 l^2/2} \int_{-\infty}^{\infty} \frac{dq_z}{2\pi} \frac{|M_{\sigma}^{i,i}(\vec{q})|^2}{q^2 + q_z^2}, \quad (2)$$

where $\vec{q} = (q_x, q_y)$, ϵ_0 is the semiconductor dielectric function and

$$M_{\sigma}^{i,i}(\vec{q}) = \int_{-\infty}^{\infty} dx \int_{-\infty}^{\infty} dz e^{iq_x x} e^{iq_z z} \times \varphi_{i,\sigma}(x + l^2 q_y/2, z) \varphi_{i,\sigma}(x - l^2 q_y/2, z). \quad (3)$$

Since the stripe states are found at relatively weak magnetic fields, we can anticipate that the valence LL which is partially occupied will not be widely separated from remote LL's. We include remote LL degrees of freedom in our calculation by accounting for the screening they produce when polarized by valence LL electrons. The random phase approximation (RPA) (one-loop) calculation, leads to the following expression for the modified dielectric function:¹⁶

$$\frac{\epsilon(\vec{q})}{\epsilon_0} = 1 - \sum'_{i',i,\sigma} \frac{n_F(\epsilon_{i',\sigma}) - n_F(\epsilon_{i,\sigma})}{2\pi l^2 (\epsilon_{i',\sigma} - \epsilon_{i,\sigma})} V_{\sigma}^{i',i}(\vec{q}) \exp(-q^2 l^2/2), \quad (4)$$

where ϵ_0 is the dielectric constant of the host semiconductor, $n_F(x)$ is a Fermi factor, the prime on the sum excludes the valence LL, and the effective inter-LL interactions $V_{\sigma}^{i',i}(\vec{q})$ differ from $V(\vec{q})$ only through the replacement of $M_{\sigma}^{i,i}(\vec{q})$ by $M_{\sigma}^{i',i}(\vec{q})$. The wave functions and single-particle eigenvalues, $\epsilon_{i,\sigma}$, used to define the effective interactions were obtained from local-spin-density self-consistent-field calculations, which include the solution of the two-dimensional single-particle Schrödinger equation that arises¹⁷ at tilted magnetic fields. The effective interactions are anisotropic because B_{\parallel} mixes the cyclotron and electric subband levels.

One-particle density matrices in a single LL, and hence also Hartree-Fock (HF) energies,¹⁸ are uniquely specified¹⁹ by the particle density function. The energy per electron of the UCDW state at fractional filling ν^* of the valence LL is given by¹⁸

$$E = \frac{1}{2\nu^*} \sum_{n=-\infty}^{\infty} \Delta_n U\left(\frac{2\pi n}{a} \hat{e}\right), \quad \Delta_n = \nu^* \frac{\sin(n\nu^* \pi)}{n\nu^* \pi}, \quad (5)$$

where a is the period of the UCDW state and \hat{e} is the direction of charge variation. The UCDW state consists of stripes of width $a\nu^*$ with occupied guiding center states separated by stripes of width $a(1-\nu^*)$ with empty guiding center states; Δ_n above is the Fourier transform of the the guiding center occupation function at wave vector $n2\pi/a$. In Hartree-Fock (HF) theory, the UCDW state energy depends only on a and \hat{e} and the optimal UCDW is obtained by

TABLE I. HF state energies per electron at $\nu^* = 1/2$ for triangular Wigner crystal, UCDW, and anisotropic Wigner crystal states. The energies are in units of $e^2/\epsilon_0 l$. These results are for zero thickness 2D electron layers and no screening.

N	e^{TWC}	a/l	e^{UCDW}	e^{AWC}
0	-0.4435	3.299		
1	-0.3443	4.443	-0.3456	-0.3509
2	-0.2897	5.805	-0.3063	-0.3091
3	-0.2667	6.890	-0.2740	-0.2764

minimizing Eq. (5) with respect these parameters. In Eq. (5), $U(\vec{q})$ can be separated into direct, $H(\vec{q})$, and exchange, $X(\vec{q})$, contributions with

$$H(\vec{q}) = \frac{1}{2\pi l^2} e^{-q^2 l^2/2} V(\vec{q})$$

$$X(\vec{q}) = - \int \frac{d^2 p}{(2\pi)^2} e^{-p^2 l^2/2} e^{i(p_x q_y - p_y q_x) l^2} V(\vec{p}). \quad (6)$$

The physics responsible for the occurrence of UCDW states is equation and robust. For an infinitely narrow electron layer the effective 2D Coulomb interaction, $V(\vec{q})$, reduces to $[L_N(q^2/2)]^2 2\pi e^2 l/\epsilon q$ where $L_N(x)$ is a Laguerre polynomial. Starting from $N=1$, zeros of $L_N(x)$ occur at smaller x with increasing N , producing a zero in the repulsive Hartree interaction at smaller wave vector where the attractive exchange interaction is stronger. In Table I we compare the $\nu^* = 1/2$ HF energies of triangular Wigner crystal states and UCDW states with maximum a satisfying $H(2\pi/a) = 0$. The triangular Wigner crystal state energy is intended to approximate the energy of possible isotropic fluid states. We see that for $N \geq 2$, the energetic preference for the UCDW states is large, substantially larger for example than the preference for Laughlin's²⁰ fluid states over Wigner crystal states at $\nu = 1/3$. These calculations suggest that for $N = 1$ the competition between isotropic fluid states and UCDW states is delicate. Also noted in Table I is the fact that in the HF approximation, the UCDW state is unstable to charge modulation along the stripes,⁸ leading to anisotropic Wigner crystal states with slightly lower energy. This instability is, however, misrepresented by the HF approximation and the system is expected^{21,8} to be effectively a UCDW at any accessible temperature for $0.4 < \nu^* < 0.6$. We appeal to the relatively small difference between UCDW and anisotropic Wigner crystal state HF energies in using the simple UCDW state to estimate the anisotropy energy.

We now turn to our evaluation for the anisotropy energy at $\nu = 5/2, 9/2$, and $13/2$ in the sample of Lilly *et al.*^{1,2} The self-consistent-field separation between lowest spin-up electrical subbands is 9.8 meV so that the valence LL's at perpendicular field for these filling factors are the spin-up $N=1, 2$, and 3 LL's of the first electrical subband, respectively. The in-plane magnetic field has only a weak effect on the LL spacing even at field-tilt angles as high as $\theta = 60^\circ$. We rep-

TABLE II. Field-tilt anisotropy energy components. Energies are per electron and in units of $10^{-4} e^2/\epsilon_0 l \sim k_B 10$ mK.

θ	No Screening			Screening			a^*/l
	$E_{A,0}^H$	$E_{A,0}^X$	E_A	$E_{A,0}^H$	$E_{A,0}^X$	E_A	
$\nu=5/2$							
20°	-32.79	36.16	1.16	-17.65	28.94	2.80	5.15
40°	-45.70	78.73	8.85	-21.26	70.63	12.38	5.24
60°	-127.32	174.73	10.73	-75.64	164.19	21.25	5.15
$\nu=9/2$							
20°	-13.52	6.17	-1.40	-5.58	7.59	0.27	6.41
40°	-43.84	18.17	-4.44	-10.83	19.51	2.23	6.41
60°	-101.57	39.78	-9.59	-15.00	47.00	8.07	6.68
$\nu=13/2$							
20°	-3.76	0.06	-0.77	-0.81	0.91	0.04	7.66
40°	-18.49	2.75	-3.48	-1.93	6.20	0.87	7.66
60°	-70.55	6.33	-12.49	-2.54	16.03	2.68	7.85

represent the effective interaction anisotropy by performing a Fourier expansion in the angle ϕ between \hat{e} and the in-plane field

$$H(q, \phi) = \sum_n H_{2n}(q) \cos(2n\phi)$$

$$X(q, \phi) = \sum_n X_{2n}(q) \cos(2n\phi), \quad (7)$$

where

$$X_{2n}(q) = - \int_0^\infty dp p H_{2n}(p) J_{2n}(pq) \quad (8)$$

and $J_m(x)$ is the Bessel function. Even at large B_{\parallel} the anisotropy of the effective interaction is relatively weak and is accurately proportional to $\cos(2\phi)$. This property of $H(\vec{q})$ is shared by $U(\vec{q})$ and greatly simplifies the UCDW energy (5) minimization procedure. For a given a the extrema of E lies either at $\phi=0$ or at $\phi=\pi/2$. We define the anisotropy energy per electron E_A as the minimum of $E(\phi=\pi/2)$ minus the minimum of $E(\phi=0)$.

Details of the anisotropy energy calculation are summarized in Table II. We first discuss the results obtained when RPA screening is neglected. Most qualitative features are already captured in a simple theory that retains only the $n=1$ leading harmonic in the UCDW energy expression and finds the optimal UCDW period $a=a_0^*$ by minimizing $H_0(2\pi/a) + X_0(2\pi/a)$. The Hartree anisotropy energy $E_{A,0}^H = -2H_2(2\pi/a_0^*)$ is consistently negative (stripes along in-plane field) but is countered by the exchange energy $E_{A,0}^X = -2X_2(2\pi/a_0^*)$. For $\nu=9/2$ and $13/2$, where the UCDW state is most robust, the Hartree term dominates when screening is neglected but exchange dominates when screening is accounted for. Our finding that the stripes prefer to be aligned perpendicular to the B_{\parallel} direction is consistent with the experimental finding^{2,4} that this is the easy transport direction. Including all harmonics in the UCDW energy ex-

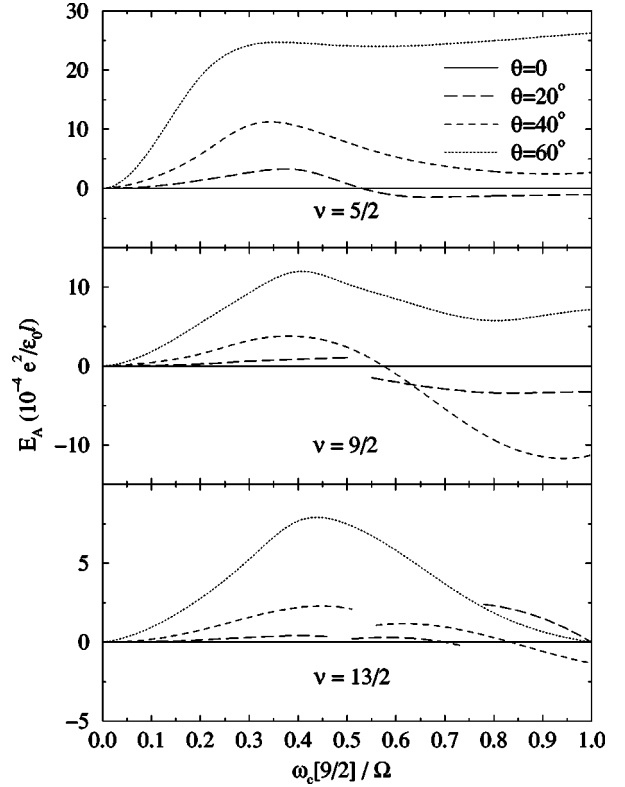


FIG. 1. Field-tilt anisotropy energy as a function of parabolic confining potential strength. Data for the valence LL close to degeneracy with another LL are not plotted as the theory fails to describe this circumstance.

pression and reoptimizing the lattice constant $a=a^*$, substantially reduces numerical value of the anisotropy energy but does not change its sign. E_A is largest in magnitude for $\nu=5/2$. Even these relatively modest anisotropy energies are sufficient to tip the delicate balance between isotropic and anisotropic states for $N=1$, explaining the transition to anisotropic states seen in experiment. We can use the calculated values for E_A to estimate the temperature below which anisotropy will be observed in the transport properties of these systems. Current experimental samples apparently have a native anisotropy of unknown origin, which can be overcome by the application of an in-plane field, reorienting the stripes and changing the easy transport direction. Since $\theta < 20^\circ$ can reorient the stripes for $N=2$ and $N=3$, we estimate from Table II that the native anisotropy energy is less than $10^{-4}(e^2/\epsilon_0 l) \sim k_B 10$ mK per electron. We can also use E_A to estimate the temperature below which anisotropy will be observed in the transport properties of these systems. Based on an experimental onset temperature $T^* \sim 100$ mK with native anisotropy we estimate that $k_B T^* \sim 10E_A$. According to our calculations the largest anisotropies occur for $N=1$ for which we predict an onset temperature exceeding 1 K at large θ . We note that our theory gives similar results for the field-tilt anisotropy energy at $\nu=11/2$ and $\nu=9/2$ and therefore as unable to explain the differences observed in the anisotropic transport measurements² in majority and minority valence LL's.

Finally, we discuss UCDW energy calculations for parabolic quantum wells with different electric subband splittings $\hbar\Omega$. The results are summarized in Fig. 1; both screening

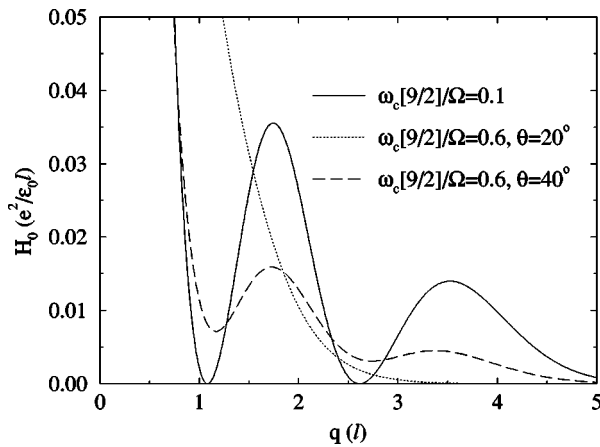


FIG. 2. Wave-vector-dependent Hartree energies for parabolic quantum well model and $\nu=9/2$.

and higher harmonics in the UCDW energy were accounted for in these calculations. The perpendicular magnetic field was chosen to correspond to the 2D electron density in the experiments of Lilly *et al.*,^{1,2} i.e., the cyclotron frequency at $\nu=9/2$ is $\hbar\omega_c[9/2]=4.24$ meV. Two regimes can be distinguished in Fig. 1. For narrow quantum wells ($\omega_c[9/2]/\Omega < 0.5$), only the lowest electrical subband is occupied at $\theta=0$, the stripes orient perpendicular to the in-plane field, and the magnitude of E_A increases with θ and decreases with N . The samples of Lilly *et al.*^{1,2} and Pan *et al.*⁴ fall into this regime. In wider quantum wells the perpendicular field va-

lence LL can belong to a higher electrical subband, and more complex behavior occurs. The solid curve in Fig. 2 shows the interaction energy H_0 for $\nu=9/2$ and a narrow parabolic quantum well. It has a structure characteristic of the $N=2$ LL effective interaction. $\{\theta$ is not indicated here as the field-tilt has a negligible effect on $H_0(q)$ for $\omega_c[9/2]/\Omega=0.1\}$. The dotted and dashed curves correspond to the case where the perpendicular field valence LL is the lowest ($N=0$) LL of the second electrical subbands. For $\theta=20^\circ$, $H_0(q)$ decreases monotonically with q , as in the perpendicular field; as explained above the UCDW is not the likely ground state for the system in this circumstance. However, at $\theta=40^\circ$, $H_0(q)$ is more akin the perpendicular field $N=2$ LL effective interaction which favors the UCDW state. This mechanism of stabilizing UCDW ground state by in-plane magnetic field is different from the one discussed above for Lilly's *et al.*^{1,2} sample and is germane to wider quantum wells with higher electrical subbands occupied. Our calculations indicate that both perpendicular and parallel orientations of the stripes with respect to the in-plane field can be realized for these tilt-induced UCDW states. The competition between isotropic and anisotropic states, and the anisotropy energy of UCDW states, will both have a complicated dependence on filling factor and tilt-angle in this regime.

The authors acknowledge stimulating interactions with J. P. Eisenstein and thank M. Fogler and R. Moessner for helpful private communications. This work was supported by NSF Grant No. DMR-9714055 and by the Grant Agency of the Czech Republic under Grant No. 202/98/0085.

- ¹M. P. Lilly *et al.*, Phys. Rev. Lett. **82**, 394 (1999).
- ²M. P. Lilly *et al.*, Phys. Rev. Lett. **83**, 824 (1999).
- ³R. R. Du *et al.*, Solid State Commun. **109**, 389 (1999).
- ⁴W. Pan *et al.*, Phys. Rev. Lett. **83**, 820 (1999).
- ⁵M. Shayegan *et al.*, cond-mat/9903405 (unpublished).
- ⁶A. A. Koukalov *et al.*, Phys. Rev. Lett. **76**, 499 (1996); Phys. Rev. B **54**, 1853 (1996); M. M. Fogler and A. A. Koukalov, *ibid.* **55**, 9326 (1997).
- ⁷R. Moessner and J. T. Chalker, Phys. Rev. B **54**, 5006 (1996).
- ⁸E. Fradkin and S. A. Kivelson, Phys. Rev. B **59**, 8065 (1999).
- ⁹H. A. Fertig, Phys. Rev. Lett. **82**, 3693 (1999).
- ¹⁰E. H. Rezayi, F. D. M. Haldane, and Kun Yang, Phys. Rev. Lett. **83**, 1219 (1999).
- ¹¹T. Stanescu, I. Martin, and P. Phillips, cond-mat/9905116 (unpublished).
- ¹²M. Fogler (private communication).
- ¹³A.H. MacDonald and U. Ekenberg, Phys. Rev. B **39**, 5959 (1989).
- ¹⁴This statement applies when mixing between different LL's is neglected.
- ¹⁵J.D. Nickila and A.H. MacDonald, Bull. Am. Phys. Soc. **34**, 914 (1989); J.D. Nickila, Ph.D. thesis, Indiana University, 1991.
- ¹⁶Because 2D and subband response is coupled in a tilted field, this is the exact RPA expression only for zero-tilt angle. The field-tilt dependence of remote LL screening is not important in our calculations, however.
- ¹⁷T.S. Lay *et al.*, Phys. Rev. B **56**, R7092 (1997).
- ¹⁸A. H. MacDonald, Phys. Rev. B **30**, 4392 (1984); A. H. MacDonald and D. B. Murray, *ibid.* **32**, 2291 (1985).
- ¹⁹A.H. MacDonald and S.M. Girvin, Phys. Rev. B **38**, 6295 (1988).
- ²⁰R.B. Laughlin, Phys. Rev. Lett. **50**, 1395 (1983).
- ²¹A.H. MacDonald and M.P.A. Fisher, cond-mat/9907278, Phys. Rev. B (to be published).